The 65th ASH Annual Meeting Abstracts

POSTER ABSTRACTS

622.LYMPHOMAS: TRANSLATIONAL-NON-GENETIC

Measuring CD8-Positive T-Cells in the Tumor Microenvironment in Classical Hodgkin Lymphoma Using Multiplex Immunofluorescence Staining and Image Analysis: A Possible Prognostic Factor

Hiromichi Takahashi, MD PhD[1], Shun Ito, MD[1], Yoko Nakanishi, PhD[2], Katsuhiro Miura, MD PhD[1], Masaru Nakagawa, MD PhD[1], Shimon Otake, MD PhD[1], Takashi Hamada, MD PhD[1], Takashi Koike, MD[1], Kazuhide Iizuka, MD PhD[3,1], Yuichi Takeuchi, MD[1], Kazuya Kurihara, MD[1], Toshihide Endo, MD[1], Hironao Nukariya, MD[1], Yoshihiro Hatta, MD[1], Shinobu Masuda, MD PhD[2], Hideki Nakamura, MD PhD[1]

[1] Department of Medicine Division of Hematology and Rheumatology, Nihon University School of Medicine, Tokyo, Japan
[2] Department of Pathology and Microbiology Division of Oncologic Pathology, Nihon University School of Medicine, Tokyo, Japan
[3] Department of Pathology and Microbiology Division of Laboratory Medicine, Nihon University School of Medicine, Tokyo, Japan

Introduction:

Classical Hodgkin lymphoma (cHL) is histologically composed of Hodgkin Reed-Sternberg (HRS) cells and the tumor microenvironment (TME) of the surrounding T-cells and macrophages, in which the expression of PD-1 and PD-L1 play critical roles in the immune response against cHL. Recently, multiplex immunofluorescence (MIF) staining and image analysis have enabled the evaluation of TME in cHL. However, the relationship between the characteristics of TME and clinical features of cHL is not fully understood. Therefore, we analyzed the pathology of patients with cHL and their clinical outcomes using MIF technology to evaluate the clinical features and the variations in TME.

Methods:

We retrospectively evaluated the clinical records and pathological samples for the diagnosis of patients with primary or relapsed cHL treated in our institution between 2010 and 2021. MIF staining and image analysis of TME were performed sequentially per the following process. Multiplexed immunofluorescence labeling against CD4, CD 8, CD30, CD68, CD163, PD-1, and PD-L1 was performed using the Opal 6-Plex Manual Detection Kit (Akoya Biosciences), and the image was captured using the Quantitative Pathology Workstation (Mantra2, Akoya). After image capture, the visual images were analyzed using supervised machine learning algorithms in Inform 2.6.0 (Akoya), which assigns phenotypes to all cells. To identify the structure of TME, the Euclidean distance from each HRS cell to other phenotype cell was calculated and identified, defined as area A within a radius of 30 μm from the HRS cells, area B from 30 μm to 60 μm, and area C from 60 μm to 120 μm. Thereafter, we analyzed the relationship between these parameters in TME at the initial diagnosis and the 3-year progression-free survival (PFS) calculated with Kaplan-Meyer methods. If the sample at the initial diagnosis was not available, the data from the sample at the first relapse were substituted.

Results:

We obtained the data from 34 patients with 45 tissues, consisting of the pathological samples at the initial diagnosis (n = 32), the first relapse (n = 12), and the second relapse (n = 1). The median patient age was 46 years (range: 16-82). In the initial diagnosis, 18 and 16 patients had localized and advanced stages, respectively. All patients were initially treated with ABVD or BV-AVD therapy. During the median observation period of 61 months, 12 patients relapsed, and the 5-year PFS rate was 73%. All 45 tissues showed the expected patterns of cellular staining, with anti-CD30 delineating cells with HRS cells, anti-CD68 with macrophages (defined as anti-CD68-only expression as M1-macrophages (M1M) and co-expression of anti-CD68 and anti-CD163 as M2-macrophages (M2M)), and CD4 positive T-cells co-expressing anti-PD-1 and macrophages co-expressing anti-PD-L1. Comparisons of the characteristics of TME among areas A, B, and C revealed that CD8-positive T-cells, PD-1-positive CD4-positive T-cells, and PD-L1-positive macrophages were significantly more common in areas A and B than in area C, whereas PD-1 negative T-cells and PD-L1 negative macrophages exhibited no particular pattern in all areas. Thus, we identified that TME structures within $60 \mu m$ are crucial for their immune effect on HRS cells. In the 34 patients at the initial diagnosis, we compared the TME within 60 μm and the PFS. As a result, TME containing higher numbers of CD8-positive T-cells (defined >15 cells) and M2M (defined > 13 cells) in TME were significantly associated with better 3-year PFS as

compared with lower numbers of these immune components (100 vs 53%, p = 0.006 and 100 vs 65%, p = 0.012, respectively), whereas such findings were negative for CD4-positive T-cells or M1M. In the TME containing >15 cells of CD8-positive T-cell, significantly more M2M (mean 16 vs 5 cells, p=0.004) and fewer (mean 16 vs 28 cells, p=0.036) PD-1-positive T-cells were observed than in the TME containing ≤15 cells of CD8-positive T-cell. In the comparisons of 32 initial and 13 relapse samples, the number of CD8-positive T-cells TME significantly decreased at the time of relapse compared to the initial diagnosis (mean 7 vs 11 cells, p = 0.035).

Conclusion:

The findings of the MIF technology suggest that CD8-positive, cytotoxic T-cell enrichment in TME is a favorable prognostic factor for cHL. Such TME could be associated with PD-1/PD-L1-independent immune response against HRS cells. These results warrant further investigations.
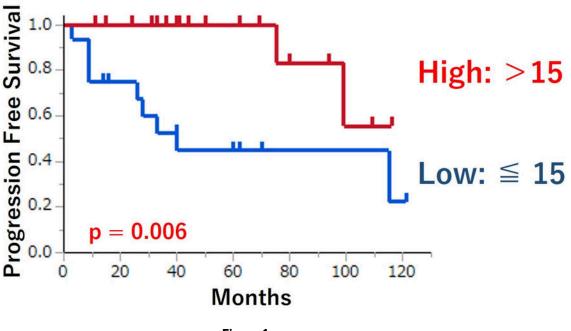
Figure 1

https://doi.org/10.1182/blood-2023-177853